CFD Letters 16, Issue 3 (2024) 96-111

CFD Letters

Journal homepage:
https://semarakilmu.com.my/journals/index.php/CFD_Letters/index
ISSN: 2180-1363

MHD Slip Flow of Upper-Convected Casson and Maxwell Nanofluid over a Porous Stretched Sheet: Impacts of Heat and Mass Transfer

V.Seethamahalakshmi[1], R.Leelavathi[2,*], T.S.Rao[3], P.Naga Santoshi[4], G.V.R.Reddy[3], Oke A.S[5]

1 Department of Mathematics, PVP Siddhartha Institute of Technology, Kanur-520007, India
2 Department of Mathematics, Koneru Lakshmaiah Education Foundation, Vaddeswaram 522302, India
3 Department of Mathematics, Koneru Lakshmaiah Education Foundation, Vaddeswaram, Guntur-522502, India
4 Department of Mathematics, Singareni Collieries Women's Degree & PG College, Kothagudem-507 101, India
5 Department of Mathematics Adekunle Ajasin University, Akungba Akoko, Nigeria

ARTICLE INFO

Article history:
Received 16 June 2023
Received in revised form 18 July 2023
Accepted 20 August 2023
Available online 12 December 2023

Keywords:
Casson fluid parameter; Upper-convected Maxwell fluid; Nanofluid; chemical reaction parameter; MHD; slip effects

ABSTRACT

The significance of this study lies in the exploration of the effects of thermal radiation and convective boundaries on magnetohydrodynamic slip flow over a nonlinear porous stretching surface. Applications range from aiding heat transfer enhancement in electronic devices and renewable energy systems to facilitating understanding in magnetic confinement fusion research and liquid metal cooling systems. The primary goal of this study is to determine how thermal radiation and convective boundaries affect the upper Maxwell Casson convected nanofluid boundary layer flow's magnetohydrodynamic slip flow over a nonlinear porous stretching surface. From the controlling PDEs, nonlinear ODEs are obtained by applying compatible similarity transformations. The quantities related to scientific and engineering concepts, such as skin friction, Sherwood number, and heat exchange, as well as other effects on momentum, temperature, and material concentration, are shown and explained in diagrams. The numerical solution of the current study and the shooting technique is achieved using the Runge-Kutta Fehelberg method. According to the results, increasing the magnetic field causes a decrease in velocity profiles. Additionally, as the velocity slip parameter increases, the local Nusselt number and the local Sherwood number fall.

1. Introduction

Potential applications of non-Newtonian fluid flow on porous stretched surfaces include bioscience, engineering, and blood flow. Casson is a shear-thinning fluid. It may show yield stress. If the applied yield stress is larger than the applied shear stress, the applied material behaves as a solid; otherwise, it behaves as a liquid and begins to move. Raju *et al.,* [1-3] and Vyakaranam *et al.,* [4] have discussed the Casson fluid application. The magnetohydrodynamic Carreau and Casson fluids' exponential heat source/sink, momentum, and thermal transport over the spinning paraboloid have all been examined by Kumaran *et al.,* [5]. As the base fluid is implanted with the silver and upper nanoparticles, Sobamowo *et al.,* [6] have examined the impacts of additional control attributes on

* *Corresponding author.*
E-mail address: drrlv2021@aliet.ac.in (R.Leelavathi)

https://doi.org/10.37934/cfdl.16.3.96111

stream and heat transfer attributes to the nanofluids. Unsteady Carreau-Casson fluids in a solution of dust and graphene nanoparticles with non-Fourier heat flux over a radiating shrinking layer have been explored by Santosh *et al.,* [7]. Santoshi *et al.,* [8] have studied the computational examination of 3D Casson-Carreau nanofluid flow. A colloidal postponement called nano fluid contains nanoparticles in a base fluid. Nanofluids have a wide range of uses in engineering, from the automotive industry to the medical sector. They are used in nuclear reactors, power plant cooling systems, geothermal energy extraction, automotive applications, electronic applications like cooling microchips, and biomedical applications like cancer therapeutics and nano cryosurgery, among other things. Due to these actual characteristics, nanofluids are relevant to the study, as shown by the references [9–14] in this debate.

The non-Newtonian fluid flow across a mixed stretchable surface has been studied with different variables by Chandra and Sandeep [15], Reddy *et al.,* [16], and Oke *et al.,* [17,18] looked at how thermal radiations affected MHD 3D flow across a stretching surface. A nano-liquid film's Eyring-Powell slip flow has been studied by Oke [19].

References [20–23] that provide more in-depth research on this subject looked at non–Newtonian Maxwell fluids under a range of physical conditions, including viscous dissipation, Newtonian heating, homogeneous–heterogeneous chemical reactions, and thermal stratification over different stretching surfaces. According to their research, temperature, and heat transmission rate both decreased as the Prandtl number increased. Abuzar *et al.,* [24] looked at how radiation and convective border restriction affected the non-Newtonian nano fluids' oblique stagnation point past the stretching layer. In consideration of the inclined stretched sheet, Yasin *et al.*, [25] numerically analysed the stagnation point flow of nanofluid. The effects of slip on MHD flow have been studied by certain researchers [26, 27] using a variety of non-Newtonian nanofluid models, such as Casson fluid and Jeffery nano-fluid, across a flexible sheet with varied physical limits. Ibrahim *et al.,* [28] investigated the influence of chemical reactions on mass and heat transfer characteristics. However, the sources covering chemical reactions and slip influences are addressed in the references [29-47]. The slip impact of MHD heat transmission of nanofluids above a stretching surface with a chemical reaction has been studied. Khan *et al.,*[48] have studied the MHD Flow and Heat Transfer of Double Stratified Micropolar Fluid over a Vertical Permeable Shrinking/Stretching Sheet with Chemical Reaction and Heat Source. Hamrelaine *et al.,* [49] investigated an Analysis of MHD Jeffery Hamel Flow with Suction/Injection by Homotopy Analysis Method. The analysis of the MHD stagnation point flow of upper-convected Maxwell fluid with chemical reaction is not considered by any of the aforementioned researchers due to the effects of nanoparticles with slip effects. Therefore, using the Runge-Kutta Fehlberg method and the shooting technique, the current paper aims to investigate the impact of nanoparticle and chemical reaction on MHD slip stagnation point flow, boundary layer flow, and heat and mass transfer of upper-convected Casson and Maxwell fluid above a stretching sheet.

The current research possesses novelty in its comprehensive investigation of non-Newtonian fluid flow over a porous stretched surface with the inclusion of various significant factors. Previous studies have explored different aspects of non-Newtonian fluids, such as Casson and Carreau fluids, with a focus on heat source/sink, momentum, and thermal transport. Additionally, nano fluids' applications in the engineering and medical sectors have been extensively studied. However, this research goes beyond previous works by combining nanoparticles, chemical reactions, and slip effects in the context of MHD slip stagnation point flow and boundary layer flow. Notably, the study specifically examines the upper-convected Casson and Maxwell fluids, incorporating the impacts of nanoparticle and chemical reactions, using advanced numerical methods like the Runge-Kutta Fehlberg method and the shooting technique. The investigation of these novel interactions in upper-convected MHD Casson and Maxwell fluids sets this research apart, contributing to a deeper understanding of complex fluid dynamics and heat transfer phenomena with potential applications in diverse fields of science and engineering. The objectives of this paper are to;

i. Explore the interactions of nanoparticles and chemical reactions in MHD slip stagnation point flow and boundary layer flow.
ii. Analyse the heat and mass transfer characteristics in the presence of slip effects in upper-convected Casson and Maxwell fluids.
iii. Utilize advanced numerical methods to obtain accurate numerical solutions for the investigated fluid dynamics and heat transfer phenomena.

2. Methodology
2.1 Mathematical Formulation

Consider the 2D motion of non-Newtonian nanofluid time-dependent and incompressible MHD slip flow of upper convected Maxwell Casson nanofluid with the thermal radiation and chemical reaction along a porous stretching surface with convective conditions. The rheological design for non-Newtonian fluid is stimulated by;

$$\tau^{\frac{1}{n}}\mu = \tau_0^{\frac{1}{n}}\mu + \dot{\gamma}^{\frac{1}{n}} \tag{1}$$

$$\tau_{ij} = \begin{cases} 2\left(\mu_B + \frac{p_z}{\sqrt{2\pi}}\right)e_{ij}, & \pi > \pi_c \\ 2\left(\mu_B + \frac{p_z}{\sqrt{2\pi}}\right)e_{ij}, & \pi < \pi_c \end{cases} \tag{2}$$

The analytical estimate of π is dependent on the non-Newtonian replica, the plastic dynamic viscosity of the non-Newtonian fluid, alongside the yield stress of the stream is denoted by π_c , μ_B, p_z respectively. Here $\pi = e_{ij}e_{ij}$ and the deformation rate (i, j) the component is e_{ij} .π is the product of part of the deformation rate with itself. The investigators have proposed the estimate for n as 1. But this estimate is more than 1 in several uses. The linear stretching produces flow. The Carreau fluid's extra stress tensor is defined as;

$$\bar{\tau}_{ij} = \eta_0\left[1 + \frac{1}{2}(n-1)(\Gamma\bar{\dot{\gamma}})^2\right]\bar{\dot{\gamma}}_{ij} \tag{3}$$

Here the extra stress tensor, zero shear rate viscosity, time constant and power-law index are denoted by $\bar{\tau}_{ij}$, η_0, Γ ,n and $\bar{\dot{\gamma}}$ is given by;

$$\bar{\dot{\gamma}} = \sqrt{\frac{1}{2}\Sigma_i \Sigma_j \bar{\dot{\gamma}}_{ij}\bar{\dot{\gamma}}_{ji}} = \sqrt{\frac{1}{2}\Pi} \tag{4}$$

Here the second invariant strain Tensor is Π . The Free stream velocity $U_e(x)$ and the stretching velocity $U_w(x)$ are of the forms $U_e(x) = ax$ and $U_w(x) = bx$ where c and d are constants. The x-axis is along the sheet and normal to the sheet y-axis is chosen. The concentration is represented by C_w

and the temperature is represented by T_w and the ambient concentration and ambient temperature are represented by C_∞ and T_∞ . Figure 1 shows the sketch of the physical model.

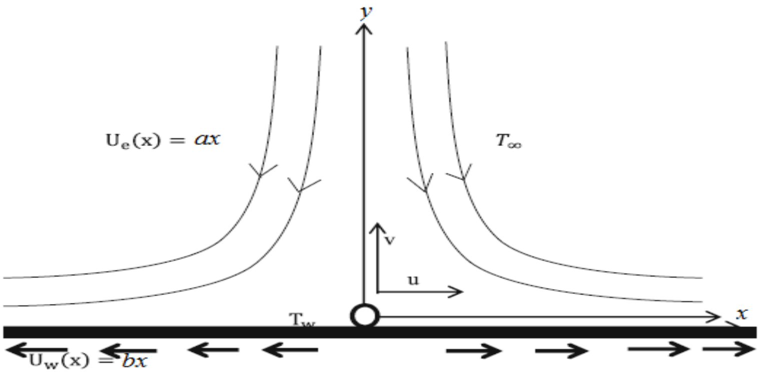

Fig. 1. Sketch of the physical model

The flow expressions are defined as:

$$\frac{\partial u}{\partial x}+\frac{\partial v}{\partial y}=0 \tag{5}$$

$$u\frac{\partial u}{\partial x}+v\frac{\partial u}{\partial y}=\begin{bmatrix}\left(1+\frac{1}{\gamma}\right)v\frac{\partial^2 u}{\partial y^2}-\varsigma\left(u^2\frac{\partial^2 u}{\partial x^2}+v^2\frac{\partial^2 u}{\partial y^2}+2uv\frac{\partial^2 u}{\partial x\partial y}\right)\\ +U_e\frac{\partial u_e}{\partial x}-\frac{\sigma B_0^2}{\rho_f}(U_e-u)-\frac{\nu}{K_1}(U_e-u)\end{bmatrix} \tag{6}$$

$$u\frac{\partial T}{\partial x}+v\frac{\partial T}{\partial y}=\alpha\frac{\partial^2 T}{\partial y^2}+\tau\left(D_B\frac{\partial C}{\partial y}\frac{\partial T}{\partial y}+\frac{D_T}{T_\infty}\left(\frac{\partial T}{\partial y}\right)^2\right)-\frac{1}{\left(\rho c_p\right)_f}\frac{\partial q_r}{\partial y}+\frac{Q_0(T-T_\infty)}{\left(\rho c_p\right)_f} \tag{7}$$

$$u\frac{\partial C}{\partial x}+v\frac{\partial C}{\partial y}=D_B\frac{\partial^2 C}{\partial y^2}+\frac{D_r}{T_\infty}\frac{\partial^2 T}{\partial y^2}-K_r\left(C-C_\infty\right) \tag{8}$$

The Navier slip conditions, convective conditions and Nield boundary conditions are assumed as follows:

$$\begin{gathered}u=U_w+A_1\frac{\partial u}{\partial y},v=0,T=T_w+A_2\frac{\partial T}{\partial y},C=C_w+A_3\frac{\partial C}{\partial y}\ \text{ at } y=0\\ u\to U_e\left(x\right)=bx,v\to 0,T\to T_\infty,C\to C_\infty\ \text{ as }\ y\to\infty\end{gathered} \tag{9}$$

where u and v are the velocity components along the x and y directions, ρ_f is the density of the base fluid, $\alpha-$ is the thermal diffusivity, ς is the relaxation time parameter of the fluid, B_0 is the strength of the magnetic field, ν is the kinematic viscosity of the fluid, K_1 is the permeability parameter, γ is the Casson fluid parameter, D_B is the Brownian diffusion coefficient, D_r is the thermophoretic diffusion coefficient, τ is the ratio between the effective heat capacity of the nanoparticle material and heat capacity of the fluid, C is the volumetric volume expansion coefficient, and ρ is the density of the particle, Kr is the chemical reaction rate, A_1, A_2, and A_3 are the velocity slip, thermal slip and concentration slip conditions respectively. The radiation heat flux (q_r) is modelled by using the Rosseland approximation given in Eq. (10).

$$q_r = -\left(\frac{4\sigma^*}{3k_1}\right)\frac{\partial T^4}{\partial y} \tag{10}$$

Here σ^* represents the constant of Stefan-Boltzmann, k_1 which gives the coefficient of mean absorption. It is also assumed that if the difference in temperature within the flow is T^4, then T^4 can be expressed as a linear combination of the temperature by expanding the T^4 by Taylor's series about T_∞ to obtain Eq. (11):

$$T^4 = T_\infty^4 + 4T_\infty^3(T - T_\infty) + 6T_\infty^2(T - T_\infty)^2 + \cdots \tag{11}$$

If we neglect the higher order beyond the first degree 1 in $\left(T - T_\infty\right)$ this series and opening brackets on the right-hand sides of Eq. (11) we obtain Eq. (12):

$$T^4 \approx -3T_\infty^4 + 4T_\infty^3 T \tag{12}$$

Substituting the right-hand side of Eq. (12) into Eq. (10) for T^4 yield Eq. (13):

$$q_r = -\left(\frac{4\sigma^*}{3k_1}\right)\frac{\partial T^4}{\partial y} = -\left(\frac{4\sigma^*}{3k_1}\right)\frac{\partial}{\partial y}(-3T_\infty^4 + 4T_\infty^3 T) = -\left(\frac{16T_\infty^3\sigma^*}{3k_1}\right)\frac{\partial T}{\partial y} \tag{13}$$

The rate of change in radiative heat flux with respect y is given by Eq. (13)

$$\frac{\partial q_r}{\partial y} = -\left(\frac{16T_\infty^3\sigma^*}{3k_1}\right)\frac{\partial^2 T}{\partial y^2} \tag{14}$$

The partial differential equations Eq. (6), Eq. (7), Eq. (8) and Eq. (14) are transformed into ordinary differential equations by introducing the dimensionless variables given by Eq. (15):

$$\psi = \sqrt{cv}\, f(\eta), \theta(\eta) = \frac{(T - T_\infty)}{(T_w - T_\infty)}, \phi(\eta) = \frac{(C - C_\infty)}{(C_w - C_\infty)}, \eta = \sqrt{\frac{c}{v}}y \tag{15}$$

The stream function velocity ψ can be defined as;

$$u = \frac{\partial \psi}{\partial y}, v = -\frac{\partial \psi}{\partial x}$$

so that Eq. (5) satisfies the continuity equation. $f(\eta)$ denote the injection and suction, η the dimensionless space variable, $\theta(\eta)$ and $\phi(\eta)$ the dimensionless of temperature and concentration of the fluid respectively.

Given the above-mentioned transformations equations Eq. (6), Eq. (7) and Eq. (8) are reduced to the following ODEs:

$$\left(1+\frac{1}{\gamma}\right)f''' + ff'' - f'^{2} + E^{2} + \left(M + 1/K\right)\left(E - f'\right) + \delta\left(2ff'f'' - f'''\right) = 0 \tag{16}$$

$$\left(1+\frac{4}{3R}\right)\theta'' + \Pr f\theta' + \Pr Nb\phi'\theta' + Nt\theta'^{2} + \Pr Q\theta = 0 \tag{17}$$

$$\phi'' + Le\phi' + \frac{Nt}{Nb}\theta'' - KrLe\phi = 0 \tag{18}$$

The transformed boundary restrictions are

$$\begin{aligned} &f(\eta) = S,\ f'(\eta) = 1 + L_1 f''(\eta), \theta(\eta) = 1 + L_2\theta'(\eta), \phi(\eta) = 1 + L_3\phi'(\eta) \quad \text{at} \quad \eta = 0 \\ &f'(\eta) \to E, \theta(\eta) \to 0, \phi(\eta) \to 0 \quad \text{as} \quad \eta \to \infty \end{aligned} \tag{19}$$

Where f' is dimensionless velocity, θ is dimensionless temperature, ϕ is dimensionless concentration, and η is the similarity variable. The prime denotes differentiation with respect to η. The skin friction C_f, local Nusselt number Nu_x and Sherwood number Sh_x are the important physical quantities they can be defined as follows:

$$C_f = \frac{\tau_w}{\rho u_w^2}, Nu_x = \frac{xq_w}{k\left(T_f - T_\infty\right)}, Sh_x = \frac{xq_m}{D_B\left(C_w - C_\infty\right)}$$

Here $\tau_w = \mu(1+\beta)\frac{\partial u}{\partial y}$ is the surface shear stress, $q_w = -k\left(\frac{\partial T}{\partial y}\right)_{y=0} + q_r$ the surface heat flux and $q_m = -D_B\left(\frac{\partial C}{\partial y}\right)_{y=0}$

Using the similarity transformation in Eq. (15) we have the following relations:

$$C_f\, Re_x^{\frac{1}{2}} = f'(0), \quad Nu_x\, Re_x^{\frac{-1}{2}} = -\left(1+\frac{4}{3R}\right)\theta'(0), \quad Sh_x\, Re_x^{\frac{-1}{2}} = -\,\phi'(0)$$

where Re_x is the local Reynolds number.

3. Numerical Solution

The R-K fourth order based on shooting technique (see Oke [50]) is used to solve the converted ODE Eq. (16) through Eq. (18) subject to the boundary constraints Eq. (19). This work emphasises the characteristics of motion, heat, and mass transmission. The field of velocity, energy, and concentration profile, as well as friction factor, Nusselt number, and Sherwood number, are all properly investigated.

4. Results and Discussion

In this section, the successive outcomes for physical variables are evaluated by using the values chosen in the references [2, 4, 9, 13] as;

$$M = 1.0, \beta = 0.1, \gamma = 0.1, Pr = 2.0, Le = 2.0, Nb = 0.1, S = 0.1,$$
$$Nt = 0.1, R = 0.1, Kr = 0.1, Q = 0.0, E = 0.1.$$

For this study, the successive outcomes for physical variables are evaluated.

Figure 2 illustrates the impact of the magnetic field's properties on the flow velocity. The magnetic parameter generates the Lorentz force, which leads to a reduction in the fluid's velocity. As the magnetic parameter values increase, the velocity profile rises, indicating a decrease in fluid velocity. For example, in the context of a conducting fluid flowing through a magnetic field, the presence of the Lorentz force may slow down the flow velocity, affecting its behaviour in the surrounding environment. Figure 3 displays the variation of velocity profiles concerning different permeability parameter values (K) that represent the presence of porous media. The inclusion of porous media increases the values of fluid flow, resulting in an acceleration of the fluid. Thus, as the permeability parameter values increase, the fluid velocity intensifies, and the fluid flow becomes more vigorous. This enhanced fluid velocity subsequently leads to the thickening of the thermal boundary layer. For instance, in the context of fluid flow through a porous material, an increase in the permeability parameter indicates the porous material's higher flow permeability, causing the fluid to flow more rapidly and leading to changes in the temperature distribution near the boundary layer.

In Figure 4, the Casson effect is observed to reduce the fluid's velocity. This reduction is due to the nature of the Casson fluid, where the yield stress decreases. As the Casson parameter increases, the yield strain is minimized, leading to an increase in the liquid's plastic dynamic viscosity. This, in turn, causes a thickening of the momentum boundary layer. Thus, in the case of a Casson fluid flowing over a surface, an increase in the Casson parameter would imply a decrease in the fluid's ability to flow easily, resulting in a decrease in its velocity and a change in the boundary layer's thickness. Figure 5 presents the temperature curves for various estimations of the thermal radiation parameter. With the upgrade in thermal radiation calculations, both the temperature profile and the thickness of the temperature boundary layer increase. For instance, in a scenario where thermal radiation is considered in a heat transfer process, an increase in the thermal radiation parameter would indicate a higher contribution of radiation heat transfer. This increased thermal radiation would lead to changes in the temperature distribution and the boundary layer thickness in the surrounding environment.

Figure 6 demonstrates how the temperature and thermal boundary layer thickness reduced when the estimations of Pr were improved and thermal diffusivity decreased, resulting in a decrease in the temperature profile. When Pr is higher, heat diffuses more slowly and more quickly than when Pr is lower, controlling the relative thickness of momentum and thermal boundary layers. Figure 7 demonstrates how the thermal boundary layers are enhanced by temperature profiles with rising Q values. The energy is released to the flow when a heat source is present. The thermal boundary layers are improved by the energy. As the thermophoresis parameter values increase, the concentration seen in Figure 7 drops.

The influence of the thermophoresis parameter on the temperature profiles is shown in Figure 8 The thermal and concentration boundary layer thickness increases as Nt increases. When the Nb concentration and temperature curves in Figures 9 and 10 increase. The thickness of the thermal boundary layer may be seen to rise at the surface. Figures 11, 12, and 13 show the impacts of the velocity ratio parameter on the stream velocity, temperature, and concentration profiles. The estimates of the velocity ratio increase the thickness of the boundary layer and the stream has a boundary layer structure. When the free flow velocity ratio equals the velocity of stretching the sheet when the velocity ratio is 1, the graph of velocity is feasible. The thickness of the thermal boundary layer, however, decreases as the velocity ratio parameter rises. The concentration profile for various Kr levels is shown in Figure 14. It has been observed that the concentration profile declined with Kr upgrading. This demonstrates that a drop in the chemical reaction parameter results in a decrease in the concentration profile by significantly thickening the concentration boundary layer. Figure 15 shows how the Lewis number affects concentration profiles. The figure shows that the concentration graph and the concentration boundary layer are thinner at higher Lewis number values. Figures 16, 17, and 18 showed how the values of L1, L2, and L3 increase as the velocity, temperature, and concentration profile decline. Figure 19 shows the characteristics of velocity profiles with changes in the suction parameter S. The output of the velocity profile increases as the values of S do.

Table 1 compares the variance of the skin coefficient to the results of another investigation for various values of the magnetic field parameter M. According to the values, our results are admirably consistent with the findings of researchers Shravani Ittedi *et al.,* [45] and Ibrahim *et al.,* [46] on a small scale. Additionally, a comparison of the heat and mass transfer rate for various values of L1 and L2 is made in Table 2 and we have discovered an admirable agreement with him to check the accuracy of the numerical solution with ShravaniIttedi *et al.,* [45] and Ibrahim *et al.,* [46]. We are therefore confident that the numerical approach is appropriate for the analysis of our issue.

Table 1
Comparison of skin friction coefficient $-f''(0)$ for different values of magnetic field parameter M when E = 0, β = 0, Le = 2.0, Pr = 2.0, and Kr = 0.1

M	ShravaniItteddi [45]	Ibrhim *et al.,* [46]	Present study
0.0	1.2104	1.2105	1.210502
0.3	1.3578	1.3578	1.357780
0.5	1.1175	1.4478	1.447569
1.0	1.6500	1.6504	1.650392

Table 2
Comparison of Nusselt number $-\theta'(0)$and Sherwood number $-\phi'(0)$for different values of thermal slip parameter L1 and concentration slip parameter L2 when E = 0, δ = 0, Le = 2.0, and Pr = 2.0

L_1	L_2	ShravaniItteddi [45]		Ibrhim *et.al.,* [46]		Present study	
		Nu	Sh	Nu	Sh	Nu	Sh
0.0	0.1	0.5721	0.5958	0.5720	0.5957	0.57205	0.59575
0.3	0.1	0.5874	0.6881	0.5873	0.6880	0.58735	0.68805
0.5	0.1	0.5125	0.7304	0.5120	0.7304	0.51225	0.73040
1.0	0.1	0.3886	0.8009	0.3886	0.8008	0.38861	0.80085
0.1	0.1	0.6810	0.7401	0.6810	0.7401	0.68100	0.74012
0.1	0.3	0.6984	0.4648	0.6984	0.4648	0.69840	0.46481
0.1	0.5	0.7062	0.3424	0.7062	0.3423	0.70621	0.34235
0.1	1.0	0.7191	0.1433	0.7190	0.1432	0.71905	0.14325

For different values of S, E, L_1 , and δ , the variation of $-f''(0)$, $-\theta'(0)$and $-\phi'(0)$is given in Table 3. From the table, we see that the skin friction coefficient increases but decreases with an increase in the velocity ratio E and the velocity slip parameter λ as the suction-injection parameter S and Deborah numberδ increase. In addition, the table shows that as the values of S and E increase and

CFD Letters
Volume 16, Issue 3 (2024) 96-111

decrease with an upsurge of Deborah number and velocity slip parameter L_1, the local Nusselt number and the local Sherwood number of the flow area.

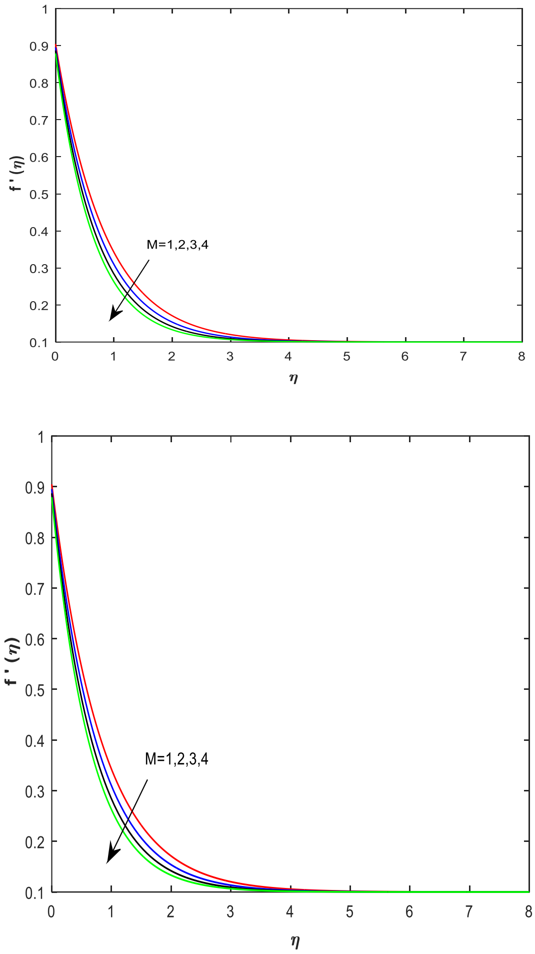

Fig. 2. Velocity profile for various values of M

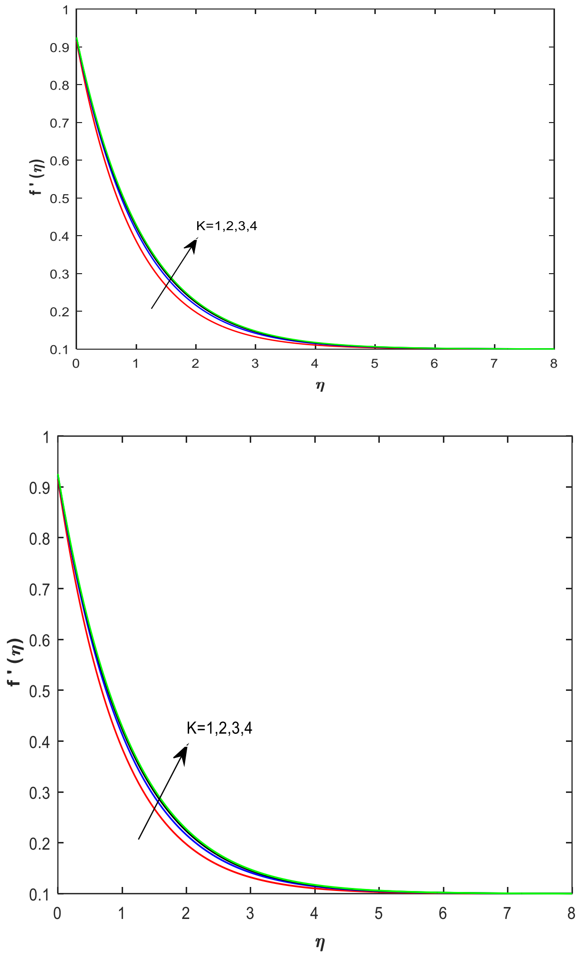

Fig. 3. Velocity profiles for various values of K

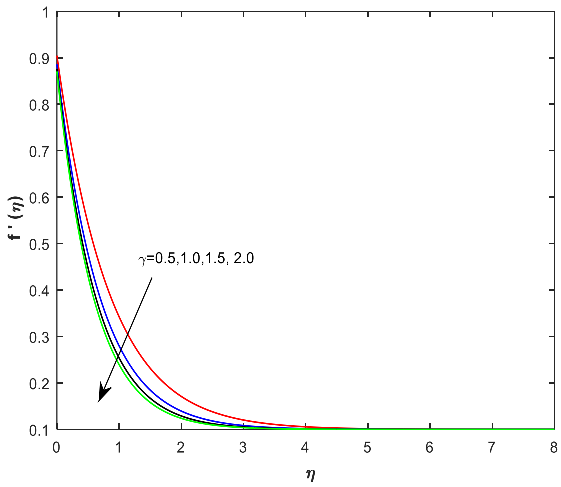

Fig. 4. Velocity profile for various values of γ

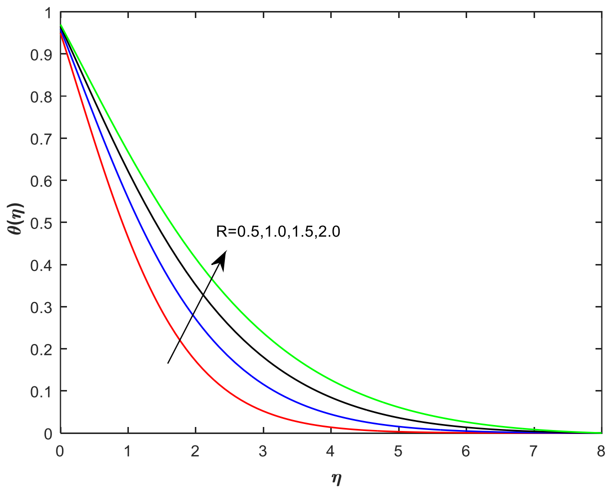

Fig. 5. Temperature profile for various values of R

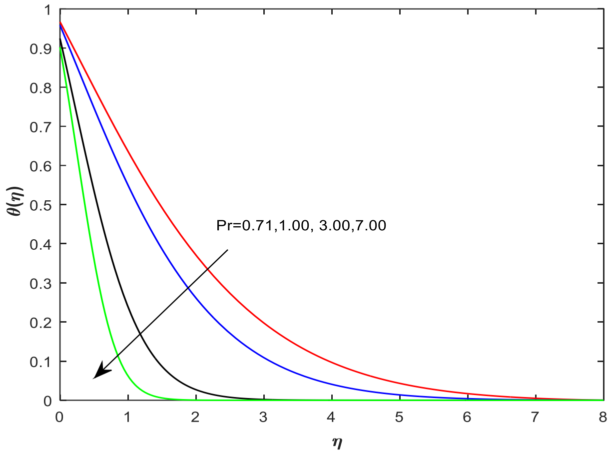

Fig. 6. Temperature Profile for various values of Pr

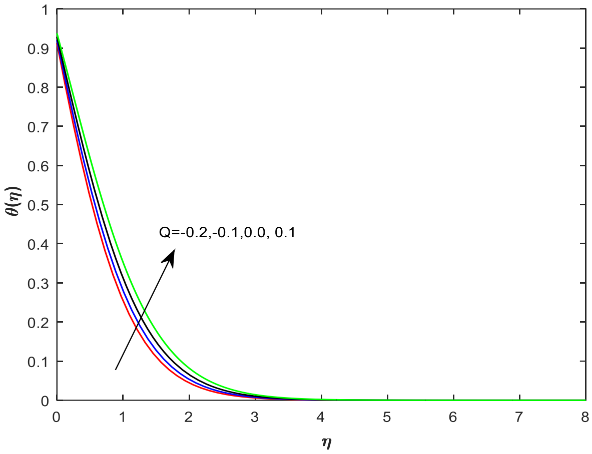

Fig. 7. Temperature profile for various values of Q

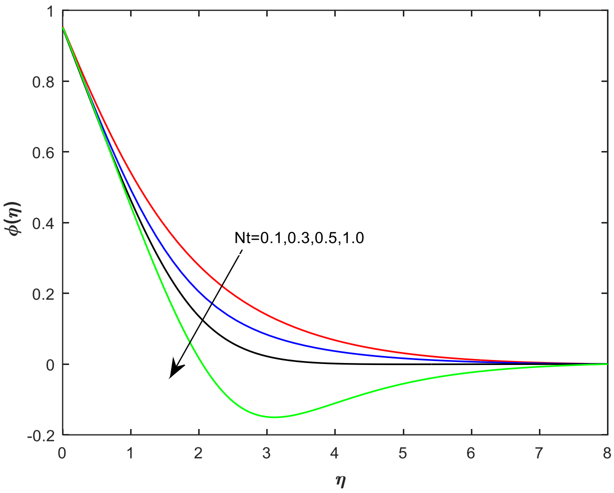

Fig. 8. Concentration profile for various values of Nt

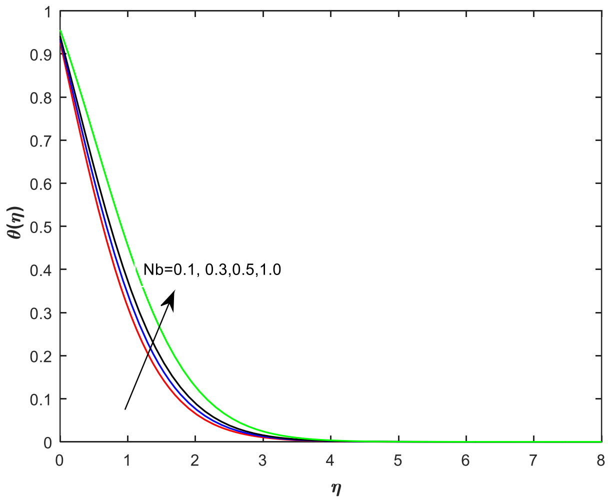

Fig. 9. Temperature profile for various values of Nb

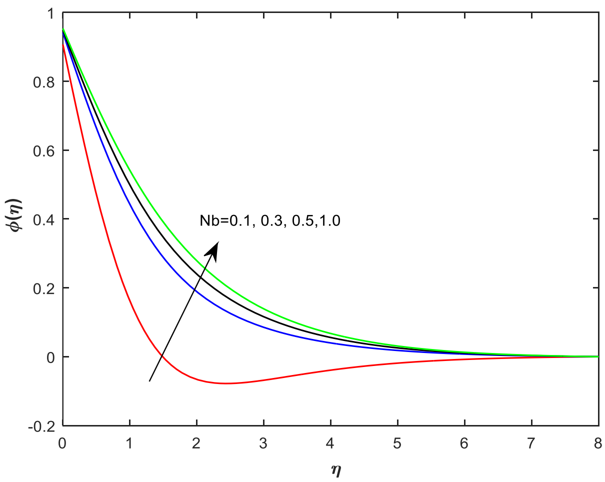

Fig. 10. Concentration profile for various values of Nb

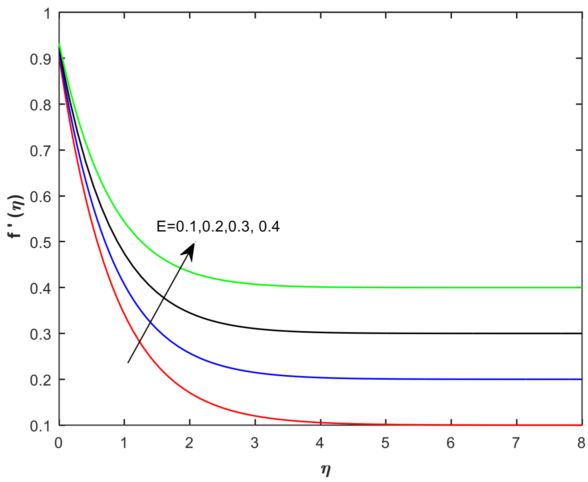

Fig. 11. Velocity profile for various values of E

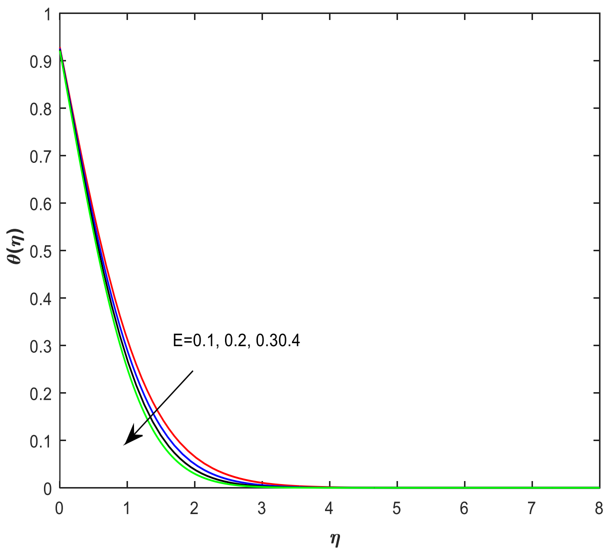

le

Fig. 12. Temperature profile for various values of E

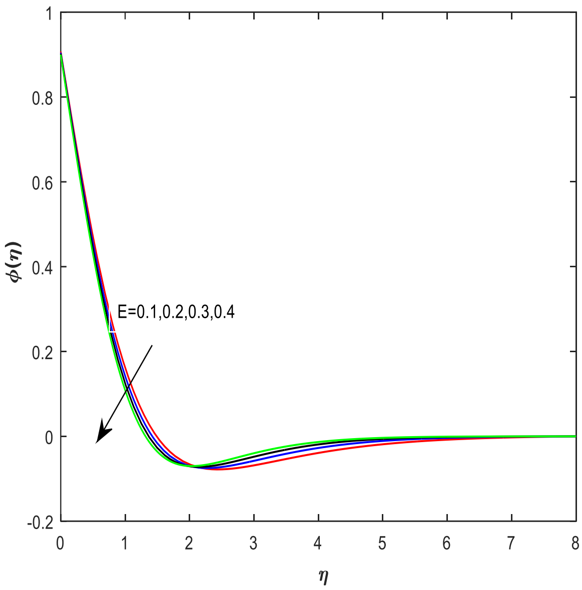

Fig. 13. Concentration profile for various values of E

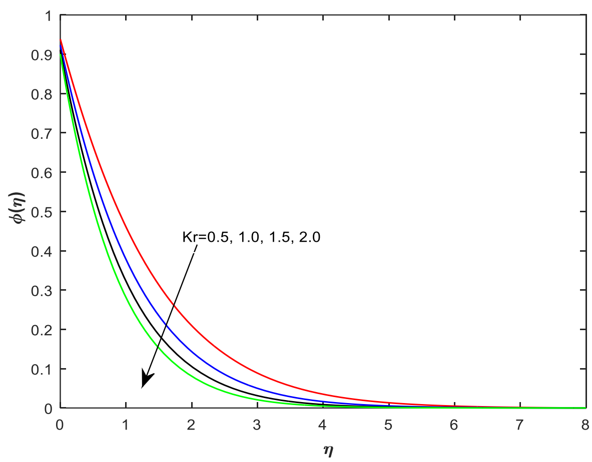

Fig. 14. Concentration profile for various values of Kr

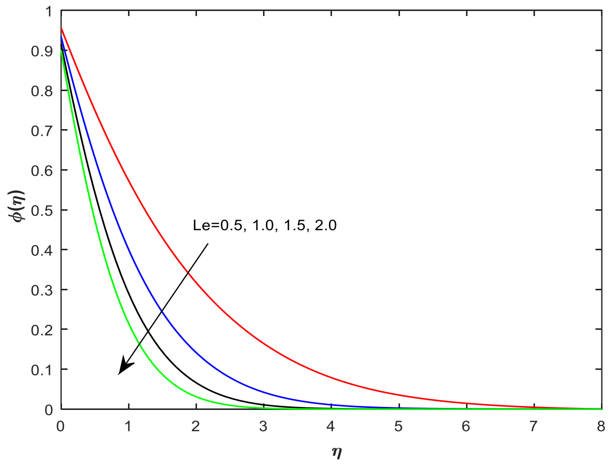

Fig. 15. Concentration profile for various values of Le

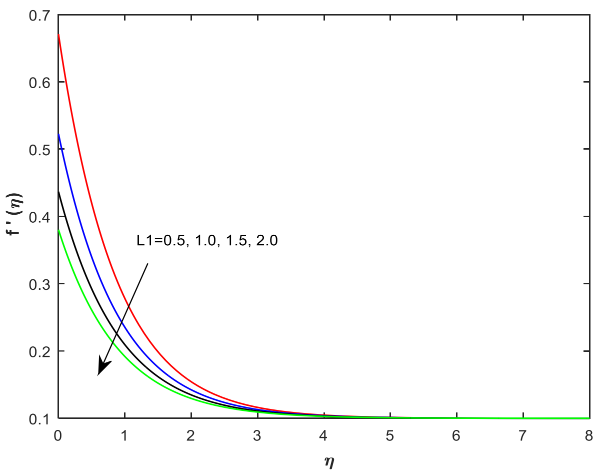

Fig. 16. Velocity profile for various values of L1

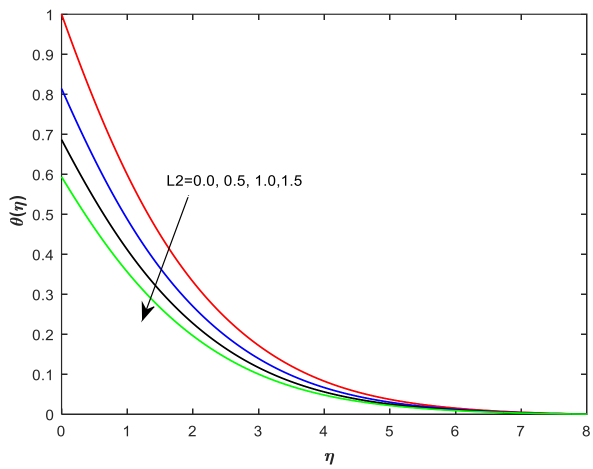

Fig. 17. Temperature profile for various values of L2

Table 3
The estimates of skin friction factor, Nusselt number, Sherwood number for different values of M, K, B, R, Pr, Q, Nt, Nb, E,Kr,Le,L1,L2,L3 for Casson fluid

B	Q	Nt	Nb	E	Kr	Le	L1	L2	L3	S	$-f''(0)$	$-\theta'(0)$	$-\phi'(0)$
0.5	0.1	0.1	0.1	0.1	0.1	0.1	0.1	0.1	0.1	0.1	0.953373	0.544371	0.755949
1											1.141696	0.557614	0.770806
1.5											1.236429	0.579709	0.795489
2											1.294181	0.624631	0.845122
0.1	-0.2	0.1	0.1	0.1	0.1	0.1	0.1	0.1	0.1	0.1	0.957216	0.623708	0.844095
	-0.1										0.957216	0.717864	0.928702
	0										0.957216	0.799163	1.002185
	0.1										0.957216	0.871248	1.067662
0.1	0	0.1	1	0.1	0.1	0.1	0.1	0.1	0.1	0.1	0.957216	0.190038	0.462225
		0.3									0.957216	0.287873	0.479390
		0.5									0.957216	0.352388	0.488595
		1									0.957216	0.439896	0.495879
0.1	0	0.1	0.1	0.1	0.1	0.1	0.1	0.1	0.1	0.1	0.957216	0.439896	0.462225
			0.3								0.957216	0.585888	0.512357
			0.5								0.957216	0.650337	0.581223
			1								0.957216	0.717864	0.928702
0.1	0	0.1	0.1	0.1	0.1	0.1	0.1	0.1	0.1	0.1	0.672554	0.717864	0.928702
				0.2							0.771461	0.744028	0.954732
				0.3							0.866380	0.767799	0.978855
				0.4							0.957216	0.789891	1.001656
0.1	0	0.1	11	0.1	0.5	0.1	0.1	0.1	0.1	0.1	0.957216	0.000001	0.614295
					1						0.957216	0.000001	0.769625
					1.5						0.957216	0.000001	0.891445
					2						0.957216	0.000002	0.993966
0.1	0	0.1	11	0.1	0.1	0.5	0.1	0.1	0.1	0.1	0.957216	0.000000	0.437074
						1					0.957216	0.000000	0.663644
						1.5					0.957216	0.000001	0.842443
						2					0.957216	0.000004	0.993947
0.1	0	0.1	11	0.1	0.1	0.5	0.5	0.1	0.1	0.1	0.309825	0.000001	0.351836
							1				0.375416	0.000002	0.361417
							1.5				0.477157	0.000002	0.375832
0.1	0	0.1	11	0.1	0.1	0.5	0.5	0	0.1	0.1	0.658061	0.000003	0.400170
								0.5			0.957216	0.000002	0.270932
								1			0.957216	0.000042	0.313497
								1.5			0.957216	0.000308	0.371921
0.1	0	0.1	11	0.1	0.1	0.5	0.5	0.1	0	0.1	0.957216	0.001246	0.457090
									0.5		0.957216	0.000042	0.313497
									1		0.957216	0.000308	0.371921
									1.5		0.957216	0.001246	0.457090
0.1	0	0.1	11	0.1	0.1	0.5	0.5	0.1	0.1	0	0.942680	0.000003	0.407666
										0.5	1.020500	0.000012	0.561738
										1	1.113429	0.000033	0.728104
										1.5	1.226358	0.000071	0.899954

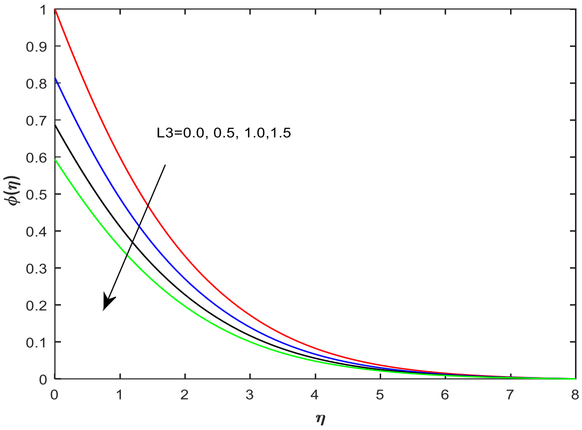

Fig. 18. Concentration profile for various values of L3

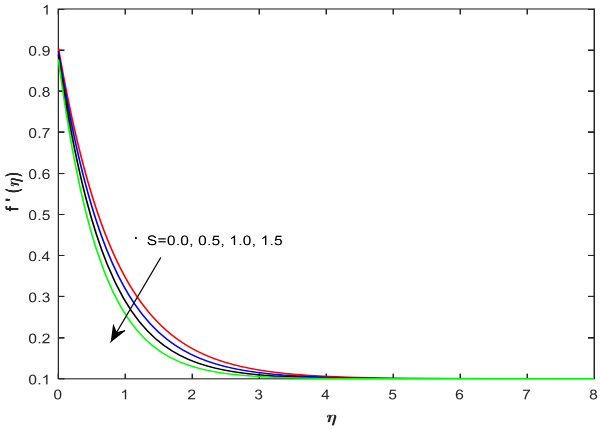

Fig. 19. Velocity profile for various values of S

5. Conclusions

This study illustrates the MHD slip effect and Casson upper convected Maxwell fluid stagnation point flow with a chemical reaction on a stretchy sheet. A similarity solution is obtained depending on the governing variables, including the velocity ratio, suction-injection parameter, Lewis numbers, Deborah number, magnetic field, Brownian motion parameter, thermophoresis parameter, chemical reactions parameter, thermal radiation parameter, velocity slip parameter, thermal slip parameter, singular slip parameter, Casson fluid parameter, and heat source parameter. The following details of the current work are displayed:

i. The effect of the magnetic field parameter's increase on the velocity field is lessened.
ii. The velocity field increases with rising thermal conductivity, while it decreases with rising solutal slip values.
iii. Concentration profiles are lowered by raising the values of Brownian motion, chemical reaction, Lewis number, thermal slip parameter, and singular slip parameter.
iv. Thermal radiation increased the thermal boundary layer's thickness.
v. The characteristics of velocity profiles with the suction parameter lead to a weakening of the velocity field.
vi. Depreciation of the velocity, temperature, and concentration profiles occurs as L1, L2, and L3 values increase.

References

[1] Raju, C. S. K., N. Sandeep, V. Sugunamma, M. Jayachandra Babu, and JV Ramana Reddy. "Heat and mass transfer in magnetohydrodynamic Casson fluid over an exponentially permeable stretching surface." *Engineering Science and Technology, an International Journal* 19, no. 1 (2016): 45-52. https://doi.org/10.1016/j.jestch.2015.05.010

[2] Raju, C. S. K., N. Sandeep, and S. Saleem. "Effects of induced magnetic field and homogeneous–heterogeneous reactions on stagnation flow of a Casson fluid." *Engineering Science and Technology, an International Journal* 19, no. 2 (2016): 875-887. https://doi.org/10.1016/j.jestch.2015.12.004

[3] Raju, C. S. K., and N. Sandeep. "Unsteady Casson nanofluid flow over a rotating cone in a rotating frame filled with ferrous nanoparticles: a numerical study." *Journal of Magnetism and Magnetic Materials* 421 (2017): 216-224. https://doi.org/10.1016/j.jmmm.2016.08.013

[4] Vyakaranam, Seethamahalakshmi Vyakaranam, Bindu Pathuri, Venkata Ramana Reddy Gurrampati, and Abayomi Samuel Oke. "Flow of Casson Nanofluid Past a Permeable Surface: Effects of Brownian Motion, Thermophoretic Diffusion and Lorenz force." *CFD Letters* 14, no. 12 (2022): 111-125. https://doi.org/10.37934/cfdl.14.12.111125

[5] Kumaran, G., N. Sandeep, and I. L. Animasaun. "Computational modeling of magnetohydrodynamic non-Newtonian fluid flow past a paraboloid of revolution." *Alexandria engineering journal* 57, no. 3 (2018): 1859-1865. https://doi.org/10.1016/j.aej.2017.03.019
[6] Sobamowo, Gbeminiyi, O. A. Adesina, and Lawrence Jayesimi. "Magnetohydrodynamic flow of dissipative casson-carreau nanofluid over a stretching sheet embedded in a porous medium under the influence of thermal radiation and variable internal heat generation." *Engineering and Applied Science Letters* 2, no. 2 (2019): 18-36. https://doi.org/10.30538/psrp-easl2019.0018
[7] Santhosh, H. B., Mahesha, and C. S. K. Raju. "Unsteady Carreau-Casson fluids over a radiated shrinking sheet in a suspension of dust and graphene nanoparticles with non-Fourier heat flux." *Nonlinear Engineering* 8, no. 1 (2019): 419-428. https://doi.org/10.1515/nleng-2017-0158
[8] Naga Santoshi, P., G. V. Ramana Reddy, and P. Padma. "Numerical scrutinization of three dimensional Casson-Carreau nano fluid flow." *Journal of Applied and Computational Mechanics* 6, no. 3 (2020): 531-542.
[9] Oke, Abayomi Samuel. "Heat and mass transfer in 3D MHD flow of EG-based ternary hybrid nanofluid over a rotating surface." *Arabian Journal for Science and Engineering* 47, no. 12 (2022): 16015-16031.
[10] Juma, Belindar A., Abayomi S. Oke, Winifred N. Mutuku, Afolabi G. Ariwayo, and Olum J. Ouru. "Dynamics of Williamson fluid over an inclined surface subject to Coriolis and Lorentz forces." *Engineering and Applied Science Letter* 5, no. 1 (2022): 37-46.
[11] Oke, Abayomi Samuel. "Combined effects of Coriolis force and nanoparticle properties on the dynamics of gold–water nanofluid across nonuniform surface." *ZAMM-Journal of Applied Mathematics and Mechanics/Zeitschrift für Angewandte Mathematik und Mechanik* 102, no. 9 (2022): e202100113. https://doi.org/10.1002/zamm.202100113
[12] Ali, Bagh, N. Ameer Ahammad, Aziz Ullah Awan, Abayomi S. Oke, ElSayed M. Tag-ElDin, Farooq Ahmed Shah, and Sonia Majeed. "The dynamics of water-based nanofluid subject to the nanoparticle's radius with a significant magnetic field: The case of rotating micropolar fluid." *Sustainability* 14, no. 17 (2022): 10474. https://doi.org/10.3390/su141710474
[13] Madhu, Macha, and Naikoti Kishan. "Finite element analysis of MHD viscoelastic nanofluid flow over a stretching sheet with radiation." *Procedia Engineering* 127 (2015): 432-439. https://doi.org/10.1016/j.proeng.2015.11.393
[14] Madhu, Macha, Naikoti Kishan, and A. Chamkha. "Boundary layer flow and heat transfer of a non-Newtonian nanofluid over a non-linearly stretching sheet." *International Journal of Numerical Methods for Heat & Fluid Flow* 26, no. 7 (2016): 2198-2217. https://doi.org/10.1108/HFF-02-2015-0066
[15] Babu, M. Jayachandra, and N. Sandeep. "MHD non-Newtonian fluid flow over a slendering stretching sheet in the presence of cross-diffusion effects." *Alexandria Engineering Journal* 55, no. 3 (2016): 2193-2201. https://doi.org/10.1016/j.aej.2016.06.009
[16] Reddy, JV Ramana, K. Anantha Kumar, V. Sugunamma, and N. Sandeep. "Effect of cross diffusion on MHD non-Newtonian fluids flow past a stretching sheet with non-uniform heat source/sink: A comparative study." *Alexandria engineering journal* 57, no. 3 (2018): 1829-1838. https://doi.org/10.1016/j.aej.2017.03.008
[17] Oke, A. S., B. C. Prasannakumara, W. N. Mutuku, RJ Punith Gowda, B. A. Juma, R. Naveen Kumar, and O. I. Bada. "Exploration of the effects of Coriolis force and thermal radiation on water-based hybrid nanofluid flow over an exponentially stretching plate." *Scientific Reports* 12, no. 1 (2022): 21733. https://doi.org/10.1038/s41598-022-21799-9
[18] Oke, A. S. "Coriolis effects on MHD flow of MEP fluid over a non-uniform surface in the presence of thermal radiation." *International Communications in Heat and Mass Transfer* 129 (2021): 105695. https://doi.org/10.1016/j.icheatmasstransfer.2021.105695
[19] Oke, A. S. "Theoretical analysis of modified eyring powell fluid flow." *Journal of the Taiwan Institute of Chemical Engineers* 132 (2022): 104152. https://doi.org/10.1016/j.jtice.2021.11.019
[20] Imran, M. A., M. B. Riaz, N. A. Shah, and A. A. Zafar. "Boundary layer flow of MHD generalized Maxwell fluid over an exponentially accelerated infinite vertical surface with slip and Newtonian heating at the boundary." *Results in physics* 8 (2018): 1061-1067. https://doi.org/10.1016/j.rinp.2018.01.036
[21] Oke, Abayomi S., Temitope Eyinla, and Belindar A. Juma. "Effect of Coriolis Force on Modified Eyring Powell Fluid flow." *Journal of Engineering Research and Reports* 24, no. 4 (2023): 26-34. https://doi.org/10.9734/jerr/2023/v24i4811
[22] Elbashbeshy, E. M. A. R., Khaled Mohamed Abdelgaber, and Hamada Galal Asker. "Heat and mass transfer of a Maxwell nanofluid over a stretching surface with variable thickness embedded in porous medium." *International Journal of Mathematics and Computational Science* 4, no. 3 (2018): 86-98.
[23] Rahbari, Alireza, Morteza Abbasi, Iman Rahimipetroudi, Bengt Sundén, Davood Domiri Ganji, and Mehdi Gholami. "Heat transfer and MHD flow of non-newtonian Maxwell fluid through a parallel plate channel: analytical and numerical solution." *Mechanical Sciences* 9, no. 1 (2018): 61-70. https://doi.org/10.5194/ms-9-61-2018

[24] Ghaffari, Abuzar, Tariq Javed, and Fotini Labropulu. "Oblique stagnation point flow of a non-Newtonian nanofluid over stretching surface with radiation: a numerical study." *Thermal Science* 21, no. 5 (2017): 2139-2153. https://doi.org/10.2298/TSCI150411163G
[25] Yasin, Abdela, Shankar Bandari, and T. Srinivasulu. "Numerical solution of stagnation point flows of nano fluid due to an inclined stretching sheet." *Int J Comput Eng Res* 8, no. 2 (2018): 2250-3005.
[26] Manjula, D., and K. Jayalakshmi. "Slip effects on unsteady MHD and heat transfer flow over a stretching sheet embedded with suction in a porous medium filled with a Jeffrey fluid." *Int J Res* 7, no. 8 (2018): 609-623.
[27] El-Aziz, Abd, and Ahmed A. Afify. "Influences of slip velocity and induced magnetic field on MHD stagnation-point flow and heat transfer of Casson fluid over a stretching sheet." *Mathematical Problems in Engineering* 2018 (2018). https://doi.org/10.1155/2018/9402836
[28] Ibrahim, S. M., G. Lorenzini, P. Vijaya Kumar, and C. S. K. Raju. "Influence of chemical reaction and heat source on dissipative MHD mixed convection flow of a Casson nanofluid over a nonlinear permeable stretching sheet." *International Journal of Heat and Mass Transfer* 111 (2017): 346-355. https://doi.org/10.1016/j.ijheatmasstransfer.2017.03.097
[29] Sreedevi, Gandluru, D. R. V. Rao, Oluwole Daniel Makinde, and G. Reddy. "Soret and Dufour effects on MHD flow with heat and mass transfer past a permeable stretching sheet in presence of thermal radiation." (2017).
[30] Dharmaiah, G., N. Vedavathi, K. S. Balamurugan, and J. Prakash. "Heat transfer on mhd nanofluid flow over a semi infinite flat plate embedded in a porous medium with radiation absorption, heat source and diffusion thermo effect." *Frontiers in Heat and Mass Transfer (FHMT)* 9, no. 1 (2017). https://doi.org/10.5098/hmt.9.38
[31] Dhanalakshmi, M., K. J. Reddy, and K. Ramakrishna. "Chemical reaction and soret effects on radiating MHD boundary layer flow over a moving vertical porous plate with heat source." *Journal of Advanced Research in Dynamical and Control Systems* 9 (2017): 2155-2166.
[32] Hymavathi, T., and W. Sridhar. "Numerical study of flow and heat transfer of casson fluid over an exponentially porous stretching surface in presence of thermal radiation." *International Journal Of Mechanical And Production Engineering Research And Development* 8, no. 4 (2018): 1145-54. https://doi.org/10.24247/ijmperdaug2018118
[33] Hari Krishna, Y., Gurrampati Venkata Ramana Reddy, and Oluwole Daniel Makinde. "Chemical reaction effect on MHD flow of casson fluid with porous stretching sheet." In *Defect and Diffusion Forum*, vol. 389, pp. 100-109. Trans Tech Publications Ltd, 2018. https://doi.org/10.4028/www.scientific.net/DDF.389.100
[34] Kumari, P. R., and D. Sree Devi. "Effect of radiation and radiation absorption on convective heat and mass transfer flow of a viscous electrically conducting fluid in a non-uniformly heated vertical channel." *International Journal of Mechanical and Production Engineering Research and Development* 8, no. Special Issue 7 (2018): 1382-1390.
[35] Kọ́rí́kọ, O. K., K. S. Adegbie, A. S. Oke, and I. L. Animasaun. "Exploration of Coriolis force on motion of air over the upper horizontal surface of a paraboloid of revolution." *Physica Scripta* 95, no. 3 (2020): 035210. https://doi.org/10.1088/1402-4896/ab4c50
[36] Juma, Belindar A., Abayomi S. Oke, Afolabi G. Ariwayo, and J. Ouru Olum. "Theoretical Analysis of MHD Williamson Flow Across a Rotating Inclined Surface." *Applied Mathematics and Computational Intelligence* 11: 133-145.
[37] Animasaun, I. L., A. S. Oke, Qasem M. Al-Mdallal, and A. M. Zidan. "Exploration of water conveying carbon nanotubes, graphene, and copper nanoparticles on impermeable stagnant and moveable walls experiencing variable temperature: thermal analysis." *Journal of Thermal Analysis and Calorimetry* 148, no. 10 (2023): 4513-4522. https://doi.org/10.1007/s10973-023-11997-6
[38] Areekara, Sujesh, A. S. Sabu, Alphonsa Mathew, and A. S. Oke. "Transport phenomena in Darcy-Forchheimer flow over a rotating disk with magnetic field and multiple slip effects: modified Buongiorno nanofluid model." *Waves in Random and Complex Media* (2023): 1-20. https://doi.org/10.1080/17455030.2023.2198611
[39] Ali, Bagh, N. Ameer Ahammad, Windarto, Abayomi S. Oke, Nehad Ali Shah, and Jae Dong Chung. "Significance of Tiny Particles of Dust and TiO2 Subject to Lorentz Force: The Case of Non-Newtonian Dusty Rotating Fluid." *Mathematics* 11, no. 4 (2023): 877. https://doi.org/10.3390/math11040877
[40] Oke, A. S., B. C. Prasannakumara, W. N. Mutuku, RJ Punith Gowda, B. A. Juma, R. Naveen Kumar, and O. I. Bada. "Exploration of the effects of Coriolis force and thermal radiation on water-based hybrid nanofluid flow over an exponentially stretching plate." *Scientific Reports* 12, no. 1 (2022): 21733. https://doi.org/10.1038/s41598-022-21799-9
[41] Reddy, G. V. R., and Y. Hari Krishna. "Soret and dufour effects on MHD micropolar fluid flow over a linearly stretching sheet, through a non-darcy porous medium." *International Journal of Applied Mechanics and Engineering* 23, no. 2 (2018): 485-502. https://doi.org/10.2478/ijame-2018-0028
[42] Arundhati, V., K. V. Chandra Sekhar, D. R. V. Prasada Rao, and G. Sreedevi. "Non-darcy convective heat and mass transfer flow through a porous medium in vertical channel with soret, dufour and chemical reaction effects." *JP Journal of Heat and Mass Transfer* 15, no. 2 (2018): 213-240. https://doi.org/10.17654/HM015020213

[43] Sekhar, KV Chandra. "Heat Transfer Analysis of Second Grade Fluid Over a Stretching Sheet Through Porous Medium Under the Influence of Chemical Reaction Parameter." *International Journal of Mechanical and Production Engineering Research and Development (IJMPERD) I* 8, no. 1 (2018): 605-612. https://doi.org/10.24247/ijmperdfeb201867

[44] Suneetha, K., S. M. Ibrahim, and GV Ramana Reddy. "Radiation and heat source effects on MHD flow over a permeable stretching sheet through porous stratum with chemical reaction." *Multidiscipline Modeling in Materials and Structures* 14, no. 5 (2018): 1101-1114. https://doi.org/10.1108/MMMS-12-2017-0159

[45] Rani, K. Sandhya, G. Venkata Ramana Reddy, and Abayomi Samuel Oke. "Significance of Cattaneo-Christov Heat Flux on Chemically Reacting Nanofluids Flow Past a Stretching Sheet with Joule Heating Effect." *CFD Letters* 15, no. 7 (2023): 31-41. https://doi.org/10.37934/cfdl.15.7.3141

[46] Ittedi, Shravani, Dodda Ramya, and Sucharitha Joga. "MHD heat transfer of nanofluids over a stretching sheet with slip effects and chemical reaction." *Int. J. Latest Eng. Res. Appl* 2, no. 08 (2017): 10-20.

[47] Ibrahim, Wubshet, and Mekonnen Negera. "MHD slip flow of upper-convected Maxwell nanofluid over a stretching sheet with chemical reaction." *Journal of the Egyptian Mathematical Society* 28, no. 1 (2020): 7. https://doi.org/10.1186/s42787-019-0057-2

[48] Khan, Ansab Azam, Khairy Zaimi, Suliadi Firdaus Sufahani, and Mohammad Ferdows. "MHD flow and heat transfer of double stratified micropolar fluid over a vertical permeable shrinking/stretching sheet with chemical reaction and heat source." *Journal of Advanced Research in Applied Sciences and Engineering Technology* 21, no. 1 (2020): 1-14. https://doi.org/10.37934/araset.21.1.114

[49] Hamrelaine, Salim, Fateh Mebarek-Oudina, and Mohamed Rafik Sari. "Analysis of MHD Jeffery Hamel flow with suction/injection by homotopy analysis method." *Journal of Advanced Research in Fluid Mechanics and Thermal Sciences* 58, no. 2 (2019): 173-186.

[50] Oke, A. S. "Convergence of differential transform method for ordinary differential equations." *Journal of Advances in Mathematics and Computer Science* 24, no. 6 (2017): 1-17. https://doi.org/10.9734/JAMCS/2017/36489